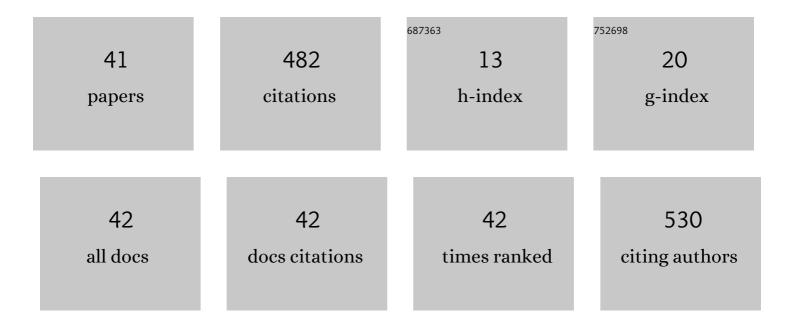
## Takahiro Ohkubo

List of Publications by Year in descending order

Source: https://exaly.com/author-pdf/1526801/publications.pdf Version: 2024-02-01



#	Article	IF	CITATIONS
1	A new universal force-field for the Li <sub>2</sub> S–P <sub>2</sub> S <sub>5</sub> system. Physical Chemistry Chemical Physics, 2022, 24, 2567-2581.	2.8	7
2	Structural analyses of amorphous calcium carbonate before and after removing strontium ions from an aqueous solution. Journal of the Ceramic Society of Japan, 2022, 130, 225-231.	1.1	3
3	Elucidating the Atomic Structures of the Gel Layer Formed during Aluminoborosilicate Glass Dissolution: An Integrated Experimental and Simulation Study. Journal of Physical Chemistry C, 2022, 126, 7999-8015.	3.1	4
4	Low melting oxide glasses prepared at a melt temperature of 500°C. Scientific Reports, 2021, 11, 214.	3.3	10
5	Examination of structure and optical properties of Ce3+-doped strontium borate glass by regression analysis. Scientific Reports, 2021, 11, 3811.	3.3	19
6	Modeling the Structure and Dynamics of Lithium Borosilicate Glasses with Ab Initio Molecular Dynamics Simulations. Journal of Physical Chemistry C, 2021, 125, 8080-8089.	3.1	17
7	Modified Li <sub>7</sub> P <sub>3</sub> S <sub>11</sub> Glass-Ceramic Electrolyte and Its Characterization. ACS Applied Materials & Interfaces, 2021, 13, 37071-37081.	8.0	12
8	Diffusion of tritiated water, 137Cs+, and 1251â^' in compacted Ca-montmorillonite: Experimental and modeling approaches. Applied Clay Science, 2021, 211, 106176.	5.2	11
9	Pore distribution of compacted Ca-montmorillonite using NMR relaxometry and cryoporometry: Comparison with Na-montmorillonite. Microporous and Mesoporous Materials, 2021, 313, 110841.	4.4	8
10	Photocatalytic hydrogen generation of monolithic porous titanium oxide-based glass–ceramics. Scientific Reports, 2020, 10, 11615.	3.3	15
11	Correlation between Structures and Physical Properties of Binary ZnO–P <sub>2</sub> O <sub>5</sub> Glasses. Physica Status Solidi (B): Basic Research, 2020, 257, 2000186.	1.5	10
12	Characterization of irradiation-induced novel voids in $\hat{I}\pm$ -quartz. AIP Advances, 2020, 10, 125212.	1.3	5
13	Densities and Refractive Indices of Molten Alkali Iodides: Estimation of Electronic Polarizability of an Iodide Ion. Journal of Chemical & Engineering Data, 2020, 65, 5240-5248.	1.9	2
14	Conduction Mechanism in 70Li <sub>2</sub> S-30P <sub>2</sub> S <sub>5</sub> Glass by Ab Initio Molecular Dynamics Simulations: Comparison with Li <sub>7</sub> P <sub>3</sub> S <sub>11</sub> Crystal. ACS Applied Materials & Interfaces, 2020, 12, 25736-25747.	8.0	12
15	Lithium conduction and the role of alkaline earth cations in Li2S–P2S5–MS (M = Ca, Sr, Ba) glasses. Journal of Non-Crystalline Solids, 2020, 538, 120025.	3.1	8
16	Temperature-Dependent Water Redistribution from Large Pores to Fine Pores after Water Uptake in Hardened Cement Paste. Journal of Advanced Concrete Technology, 2020, 18, 588-599.	1.8	13
17	Activity Report on Information-Gathering of Database Literatures for Molten Salts. Electrochemistry, 2020, 88, 243-252.	1.4	2
18	X-ray absorption near-edge structure of Ag cations in phosphate glasses for radiophotoluminescence applications. Journal of the Ceramic Society of Japan, 2019, 127, 924-930.	1.1	9

ΤΑΚΑΗΙRΟ ΟΗΚUBO

#	Article	IF	CITATIONS
19	Correlation between emission properties, valence states of Ce and chemical compositions of alkaline earth borate glasses. Journal of Luminescence, 2018, 197, 98-103.	3.1	12
20	Li conduction pathways in solid-state electrolytes: Insights from dynamics and polarizability. Chemical Physics Letters, 2018, 698, 234-239.	2.6	9
21	Molecular Dynamics Simulation of Water Confinement in Disordered Aluminosilicate Subnanopores. Scientific Reports, 2018, 8, 3761.	3.3	17
22	Molecular Dynamics Simulations of the Thermal and Transport Properties of Molten NaNO <sub>2</sub> –NaNO <sub>3</sub> Systems. Electrochemistry, 2018, 86, 104-108.	1.4	3
23	New Insights into the Cs Adsorption on Montmorillonite Clay from 133Cs Solid-State NMR and Density Functional Theory Calculations. Journal of Physical Chemistry A, 2018, 122, 9326-9337.	2.5	13
24	Magnesiothermic Reduction of Silicon Dioxide to Obtain Fine Silicon Powder in Molten Salt Media: Analysis of Reduction Mechanism. Electrochemistry, 2018, 86, 198-201.	1.4	8
25	Insights from abÂinitio molecular dynamics simulations for a multicomponent oxide glass. Journal of the American Ceramic Society, 2018, 101, 1122-1134.	3.8	21
26	Formation of metallic cation-oxygen network for anomalous thermal expansion coefficients in binary phosphate glass. Nature Communications, 2017, 8, 15449.	12.8	42
27	Electronic Polarisability of NaNO <sub>2</sub> –NaNO <sub>3</sub> and NaOH–NaNO <sub>3</sub> Ionic Melts and Effective Ionic Radius of OH <sup>ï¼</sup> . Zeitschrift Fur Naturforschung - Section A Journal of Physical Sciences, 2017, 72, 71-76.	1.5	1
28	Electrical Conductivity of Molten DyCl3-NaCl and DyCl3-KCl Systems: An Approach to Structural Interpretations of Rare Earth Chloride Melts. Zeitschrift Fur Naturforschung - Section A Journal of Physical Sciences, 2017, 72, 1105-1112.	1.5	0
29	<i>Ab Initio</i> Molecular Dynamics Simulations and GIPAW NMR Calculations of a Lithium Borate Glass Melt. Journal of Physical Chemistry B, 2016, 120, 3582-3590.	2.6	15
30	Pore distribution of water-saturated compacted clay using NMR relaxometry and freezing temperature depression; effects of density and salt concentration. Applied Clay Science, 2016, 123, 148-155.	5.2	33
31	An adaptive finite-element method for large-scale ab initio molecular dynamics simulations. Physical Chemistry Chemical Physics, 2015, 17, 31444-31452.	2.8	18
32	Changes in surface structure of sodium aluminoborosilicate glasses during aqueous corrosion analyzed by using NMR. Journal of Physics and Chemistry of Solids, 2015, 77, 164-171.	4.0	6
33	Time-dependent Born charges of lithium borate melts by ab initio molecular dynamics. Chemical Physics Letters, 2014, 612, 68-72.	2.6	1
34	First-Principles Molecular Dynamics Simulation and Conductivity Measurements of a Molten xLi2O–(1) Tj ETQo	0 0 0 rgB	Г /Qyerlock I
35	The Local Structure of Liquid TiCl4 Analyzed by X-Ray Diffraction and Raman Spectroscopy. Zeitschrift Fur Naturforschung - Section A Journal of Physical Sciences, 2013, 68, 66-72.	1.5	2

<sup>36</sup>Deconvolution and Estimation of Water Diffusion in Sulfonated Polyethersulfone Membranes Using<br/>Diffusion-Weighted Inversion Recovery.. Journal of Physical Chemistry Letters, 2012, 3, 1030-1034.4.611

Таканіго Онкиво

#	Article	IF	CITATIONS
37	Self-diffusion coefficient of lithium in molten xLi2O–(1â^'x)B2O3 system using high-temperature PFG NMR. Chemical Physics Letters, 2012, 530, 61-63.	2.6	8
38	Molecular dynamics simulations of nafion and sulfonated poly ether sulfone membranes II. Dynamic properties of water and hydronium. Journal of Molecular Modeling, 2012, 18, 533-540.	1.8	20
39	Molecular dynamics simulations of Nafion and sulfonated polyether sulfone membranes. I. Effect of hydration on aqueous phase structure. Journal of Molecular Modeling, 2011, 17, 739-755.	1.8	26
40	Understanding properties of copoly(arylene ether nitrile)s high-performance polymer electrolyte membranes for fuel cells from molecular dynamics simulations. Theoretical Chemistry Accounts, 2011, 130, 555-561.	1.4	3
41	An approach of NMR relaxometry for understanding water in saturated compacted bentonite. Physics and Chemistry of the Earth, 2008, 33, S169-S176.	2.9	29